Dynamics of Atmospheres and Oceans 53–54 (2012) 17–35

Contents lists available at SciVerse ScienceDirect

Dynamics of Atmospheres and Oceans

journal homepage: www.elsevier.com/locate/dynatmoce

The Makassar Strait pycnocline variability at 20–40 days

Kandaga Pujiana[a,d,*], Arnold L. Gordon[a], E. Joseph Metzger[b], Amy L. Ffield[c]

[a] Lamont-Doherty Earth Observatory, Palisades, NY, United States
[b] Naval Research Laboratory, Stennis Space Center, MS, United States
[c] Earth & Space Research, Upper Grandview, NY, United States
[d] Faculty of Earth Sciences and Technology at Bandung Institute of Technology, Bandung, West Java, Indonesia

ARTICLE INFO

Article history:
Received 28 May 2011
Received in revised form 1 December 2011
Accepted 5 January 2012
Available online 14 January 2012

Keywords:
Makassar Strait
Indonesian throughflow
Intraseasonal variability
Eddies, eddy-resolving model

ABSTRACT

The characteristics and plausible genesis of the 20–40 day variability observed within the Labani Channel, a constriction within the Makassar Strait, Indonesia, are described. The 20–40 day variability, trapped beneath the depth of the strongest stratification of the pycnocline, is most evident in the across-strait flow, and in the across-strait gradient of the along-strait flow as well as in the vertical displacements of isotherms. The 20–40 day energy distribution of the across-strait flow is identifiable as a blue spectrum, demonstrating downward phase propagation. The flow fields are approximated by a vortex velocity structure, and the corresponding isotherm displacements imply potential vorticity conservation. We propose that the 20–40 day features observed in the Labani Channel are expressions of cyclonic and anti-cyclonic eddies that are advected southward within the Makassar Strait throughflow. Analysis of simulated eddy kinetic energy from an eddy-resolving model further indicates that the upstream instability of the background flow within Makassar Strait is the energy source for the eddies which are dissipated within the Labani Channel.

1. Introduction

Makassar Strait is the primary Pacific water inflow gateway to the Indonesian throughflow [ITF] (Fig. 1a; Gordon and Fine, 1996). Observations made during 2004–2006 indicated that the Makassar Strait throughflow contributed 12×10^6 m^3/s to the ITF total of 15×10^6 m^3/s (Gordon et al., 2008,

* Corresponding author at: Lamont-Doherty Earth Observatory, 61 Route 9W, Palisades, NY 10964, United States. Tel.: +1 845 365 8608; fax: +1 845 365 8175.
E-mail address: kandaga@ldeo.columbia.edu (K. Pujiana).

0377-0265/$ – see front matter © 2012 Elsevier B.V. All rights reserved.
doi:10.1016/j.dynatmoce.2012.01.001

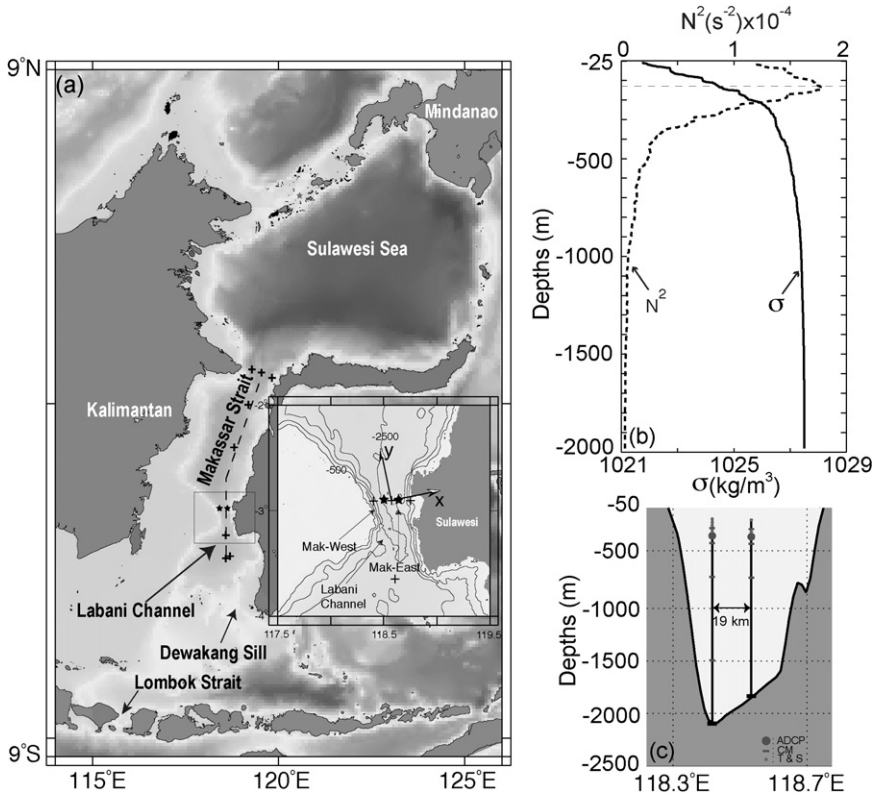

Fig. 1. (a) Locations of point measurements in Makassar Strait. The moorings are shown as stars and are deployed in the Labani Channel, a constriction in Makassar Strait. Crosses denote CTD casts during 1996–1998. Inset displays an expanded view of the Labani Channel, the major and minor axes of the channel, and the mooring sites (Mak-West and Mak-East). The along-strait axis (y) and across-strait axis (x) is tilted 10° counterclockwise relative to the geographic north and east respectively. (b) The average vertical structure of the interior Makassar Strait inferred from several CTD casts during 1993–1998 given in Fig. 1. The average of potential density (σ, solid line) and buoyancy frequency (N^2, dashed line). (c) A schematic of the mooring configuration deployed across the Labani Channel.

2010). The Makassar Strait throughflow is not steady but rich in interannual and seasonal variability as well as energetic fluctuations at tidal and intraseasonal [<90 day period] timescales (Gordon et al., 2010).

An earlier investigation of intraseasonal flow in Makassar Strait, using a 1.5 year (1996–1998) time series of along-channel speeds at 300 m and 450 m, showed two significant intraseasonal variability [ISV] peaks: 35–60 and 70–100 days (Susanto et al., 2000). Estimates based on numerical experiments suggested that the two peaks were directly linked to remote forcing emanating in the Western Pacific and Indian Ocean, as well as baroclinic eddies originating in the Sulawesi Sea (Qiu et al., 1999; Masumoto et al., 2001). The *International Nusantara Stratification and Transport* [INSTANT] program from 2004 to 2006 (Sprintall et al., 2004; Gordon and Kamenkovich, 2010) provides a longer time series with improved vertical resolution of the Makassar Strait throughflow. The Makassar along-strait flow observed by the INSTANT program reveal that the 45–90 days variability characterizes the intraseasonal motions in the Makassar Strait pycnocline, and the vertical structure of the motions resembles that of remotely forced baroclinic waves (Pujiana et al., 2009).

In this study we investigate the 20–40 day signatures within the Makassar Strait pycnocline and focus the analysis on the across-strait flow (a parameter that has been overlooked in previous studies), relative vorticity derived from the along-strait flow at the two INSTANT moorings located across Makassar Strait and the temperature fluctuations. Although the across-strait mean flow in Makassar

Strait is smaller than the along-strait mean flow (the maximum across-strait mean flow at the Labani Channel $\sim O(0.25\,\mathrm{cm/s})$), its variance exhibits some interesting aspects. For example, the flow fields at periods of 20–40 days show that the variances in the across-strait component are comparable or larger than that in the along-strait direction at depths ranging from 100 to 300 m in the Makassar Strait pycnocline. We propose that the pronounced 20–40 day variability in the Makassar Strait pycnocline derives its momentum from cyclonic and anti-cyclonic eddies, which are advected southward with the mean Makassar Strait throughflow. A better understanding on the 20–40 day features provides a fuller picture of Makassar Strait intraseasonal flow.

The presentation of this paper is organized as follows. We will first describe the data employed in Section 2. Section 3 covers general descriptions of the 20–40 day variability and their corresponding eddy characteristics from several parameters observed in the Labani Channel. This is then followed by discussion on the eddy genesis in Makassar Strait as simulated by an eddy-resolving model in Section 4. The last section concludes the paper with Section 5.

2. Data

The INSTANT program observed the ITF by means of moorings with ADCPs, current meters, and temperature sensors, deployed at several Indonesian passages linking the Pacific to the Indian Ocean (Sprintall et al., 2004). For this study we will be using the INSTANT data within Makassar Strait. We also utilize several Conductivity, Temperature, Depth [CTD] casts from the Arus Lintas Indonesia [ARLINDO] program of 1993–1998 (Gordon and Susanto, 1999) and simulated velocity vectors from the HYbrid Coordinate Ocean Model [HYCOM] (Metzger et al., 2010).

2.1. ADCP and current meter

The INSTANT 2004–2006 program monitored the ITF transport in Makassar Strait from two moorings: 2°51.9′ S, 118° 27.3 E [MAK-West] and 2°51.5′ S, 118° 37.7′ E [MAK-East], within the 45 km wide Labani Channel (Gordon et al., 2008; Fig. 1a). Each mooring consisted of an upward-looking RD Instruments Long Ranger 75 kHz Acoustic Doppler Current Profiler [ADCP] at a depth of 300 m and four current meters deployed at 200, 400, 750, and 1500 m (Fig. 1c). The Mak-West and Mak-East moorings recorded ∼3-year long datasets from 2004 to late 2006. The datasets, horizontal velocity vectors, are linearly interpolated onto a 25-m depth grid for each two-hour time step to produce gridded current vectors from 50 to 450 m of water column. The gridded horizontal current vectors are subsequently projected to the along (y) and across-strait (x) axis of the Labani Channel, which are oriented along −10° and 80° (relative to north and positive is clockwise) respectively (Fig. 1a), to yield gridded along (v) and across-strait (u) currents.

2.2. CTD

The CTD datasets used for this study are a compilation of several CTD casts collected within or near Labani Channel during ARLINDO 1993–1998 cruises (Fig. 1a). For each station, a Neil Brown Instrument System Mark III [NBIS MK III] CTD measured conductivity, temperature and pressure within 12 h period, yielding CTD casts or temporal variability of measured parameters. CTD was lowered at a rate of 1 $\mathrm{ms^{-1}}$, and a 16 $\mathrm{s^{-1}}$ sampling rate was selected. A phase lagging filter is applied to the conductivity data as correction for the time constant mismatch. The data are then coarsely de-spiked and reduced to a 1-dbar pressure series by applying a 5-scan median filter around the target pressures.

A density profile inferred from several CTD casts within the Labani Channel shows that the pycnocline layer occupies a small fraction of water column from ∼25 to 450 m, with the strongest stratification at mid-pycnocline near 125 m separating the upper (25–100 m) and lower (150–450 m) pycnocline (Fig. 1b).

2.3. Temperature sensors

Several temperature and pressure sensors attached to Mak-West and Mak-East moorings measured the temporal variability of the temperature profile in Makassar Strait. Mak-West mooring provided

better temperature profile resolution with 17 sensors attached at different levels from 100 m to 400 m; Mak-East mooring only had 5 sensors. The sensors sampled temperature and pressure at 6-min intervals over a period of almost 3 years from January 2004 to November 2006. The temperature datasets are linearly interpolated onto a 25-m depth grid for each two-hour time step to provide the gridded temperature data from 150 to 350 m of water column. Since the vertical structure of temperature variability is less resolved at Mak-East mooring, we will only analyze the temperature profile datasets from Mak-West.

To investigate the vertical structure of thermal field, mooring sensor temperature data available in the lower pycnocline layer are converted to vertical displacement (η). Neglecting horizontal advection, diffusion, and heat sources, η is calculated using a heat equation, which is simply a ratio between the gridded temperature amplitudes and the vertical gradient of the averaged temperature, $\eta(z,t) = T(z,t)/\partial T/\partial z$, where z and t denote depth and time respectively. The averaged temperature is a mean of the entire ~3-year datasets. To remove the static stability effect from η, we normalize η with the ratio between stratification frequency structure (determined from the CTD data shown in Fig. 1b) and its corresponding vertical average, $\eta_n(z,t) = \eta(z,t)\,[N/N_o]$, where subscript n and o are for normalized and vertically averaged respectively.

2.4. Simulated data

Simulated velocity vectors and temperature variability from a numerical ocean model are also used in this study. HYCOM has a horizontal resolution of $1/12.5^\circ \cos(\text{lat}) \times 1/12.5^\circ$ and employs 32 hybrid vertical coordinate surfaces with potential density referenced to 2000 m. It has been shown to realistically simulate the circulation pathways of the Indonesian Seas, and specific model formulation details can be found in Metzger et al. (2010). We examine daily data for a 3-year period from 2004 to 2006 within the Makassar Strait pycnocline, where the data are gridded vertically with a uniform resolution of 25 m from the surface to 450 m of water column.

3. Description of the intraseasonal velocity and thermal fields

In this section, general characteristics of the Labani Channel velocity and temperature profile variability measured are described. The statistical methods used to explore those characteristics are mainly spectral method, cross-correlation in frequency domain, and complex principal component analysis.

3.1. Observation

3.1.1. Horizontal and sheared flows

Gordon et al. (2008) using INSTANT data from 2004 to 2006 reported the vertical and horizontal profiles of the Makassar Strait mean flow for sub-tidal variability and found that $\bar{v}$ revealed a distinct maximum southward ($-y$) speed at 140 m with western intensification. The average direction of the flow points slightly to the east of approximately north-south along-axis direction. Superimposed on the mean flow are the fluctuations (u' and v') across a broad spectrum from inertial to interannual time frame. Focusing on the intraseasonal variability and investigating the vertical profile of the variance attributed to along-strait and across-strait flow, $\overline{u'^2}$ and $\overline{v'^2}$, where over bar delineates integration over intraseasonal periods, we find that the profile exhibits: the maximum $\overline{u'^2}$ is found at mid pycnocline (Fig. 2a), while $\overline{v'^2}$ attains maximum magnitude at depth closer to the sea surface (Fig. 2b). The ratio between $\overline{u'^2}$ and $\overline{v'^2}$ suggests that the intraseasonal motions are anisotropic throughout the Mak-West pycnocline depths (Fig. 2c), and $\overline{u'^2} > \overline{v'^2}$ for $75 \leq z \leq 225$ m. If the ratio were derived for motions with periods of 20–40 days only, the depths where $\overline{u'^2} > \overline{v'^2}$ would then extend from 75 to 275 m (not shown). Meanwhile Mak-East mooring shows that $\overline{u'^2} > \overline{v'^2}$ is restricted to a thinner water column from 100 to 150 m (Fig. 2c).

The structure of variances for both velocity components versus depths (Fig. 2) likely reflects the dynamics of the intraseasonal motions at the Labani Channel. For example, a topographically trapped

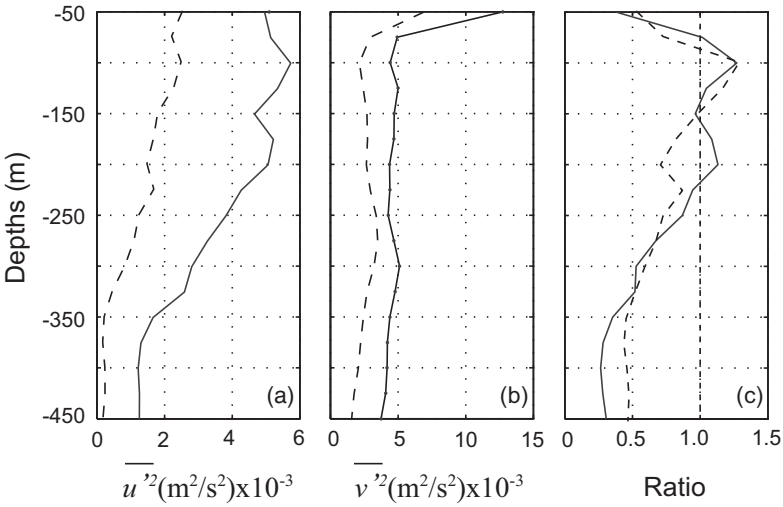

Fig. 2. Profiles of variances attributed to u' (a) and v' (b) at intraseasonal timescales (20–90 days) within the Mak-West (solid line) and Mak-East (dashed line) thermocline. The corresponding ratio between u and v for each mooring (solid line: Mak-West; dashed line: Mak-East) is given in (c).

baroclinic Kelvin wave, a forcing that theoretically requires small transverse flow, may explain stronger signatures of $v'(z)$ at depths beneath 225 m. An analysis of v' at intraseasonal periods over pycnocline depths in Makassar and Lombok Straits suggests that remotely forced baroclinic waves propagate from Lombok to Makassar Strait in the lower pycnocline depths (Pujiana et al., 2009). On the other hand, robust signatures of u' at intraseasonal timescales over depths of 75–225 m maybe driven by a topographic Rossby wave or an advected eddy whose dominant signal is expected to be in the normal component or x-direction at the Labani Channel.

A spectral analysis is applied to the datasets to examine which periods within intraseasonal timescales dominate the flow field variances in the Makassar Strait pycnocline. The power spectrum is computed using the multi-taper method with adaptive weighing. Two distinct spectral peaks, 20–40 days and 45–90 days, generally characterize the intraseasonal flows in the Makassar Strait pycnocline. The 45–90 day variability is a dominant feature in v' for throughout the pycnocline depths and extracts most of its energy from remotely forced baroclinic waves (Pujiana et al., 2009).

As for the 20–40 day variability, v' shows strong signature at 100–150 m of the Mak-West water column, where the flow is well defined by a spectral peak centered at 30-day (Fig. 3a). A distinct monthly spectral peak is absent beneath 150 m of the Mak-West pycnocline although the 20–40 day variability energy does not change substantially with depth. Some discrepancies are found from the Mak-East pycnocline, however, in which the spectral peak centered at a shorter period of 25-day is more dominant and occurs deeper in the lower pycnocline from 225 to 300 m (Fig. 3b). Furthermore, relative vorticity (ζ') computed from v' of both moorings, shows significant variance associated with monthly variation. A broad spectral peak of 20–40 day centered at a period of 30-day characterizes ζ' at depths that extend from the base of the upper pycnocline to the lower pycnocline layer, and its energy is comparable or larger than that attributed to the 45–90 day variability (Fig. 3c).

The signature of the 20–40 day variability over the Makassar Strait pycnocline is more pronounced in the u' data. The vertical distribution of energy density of u' at Mak-West across intraseasonal frequencies for several depths (Fig. 4a) indicates that the spectrum shape transforms from red to blue spectrum as depth increases from 100 to 175 m; a blue spectrum with a distinct spectral peak centered at 25-day gains energy with depth. Deeper in the lower pycnocline, the spectral peak of the 20–40 day variability tends to be centered at a longer period of 30-day. The Mak-East mooring also shows a similar pattern of the 20–40 day variability in the lower pycnocline (Fig. 4b). The 20–40 day variation observed from the Mak-East is also linked to that observed from the Mak-West as

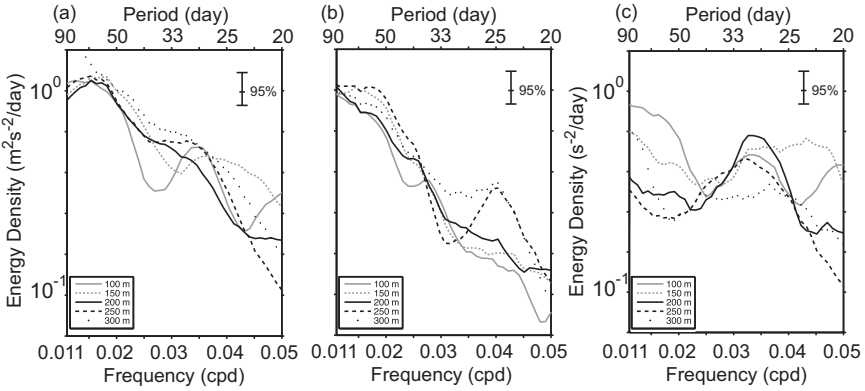

Fig. 3. Multitaper spectral estimates of v' observed at different levels in the Mak-West (a) and Mak-East (b) lower thermocline during 2004–2006. (c) Displays spectral estimates of across-strait gradient of v', computed by subtracting v' observed at Mak-East from that observed at Mak-West. Error bars on the spectral estimates mark the 95% confidence limits.

more than 80% of variance attributed to the 20–40 day variability from both mooring is statistically coherent. In addition to being coherent, the 20–40 day variability from the two moorings does not exhibit a significantly different from zero phase shift, a fact which may indicate that the 20–40 day variability has its horizontal scale across the strait larger than the ∼19 km distance separating the moorings.

Distinct 20–40 day spectral peaks marking u' and ζ' may express turbulent fluctuations on the mean flow that transports momentum across the strait. The instantaneous rate of along-strait momentum transfer in the across-strait direction is defined as $\rho_o(V+v')u'$, where V is the mean flow, and u' and v' are velocity fluctuations in the across-strait and along-strait directions respectively. The average rate of flow of along-strait momentum in the across-strait direction is therefore $\rho_o\overline{(V+v')u'} = \rho_o V\overline{u'} + \rho_o\overline{v'u'}$ as $\overline{u'} = 0$. The Reynolds stress, $\rho_o\overline{v'u'}$, is approximated with a cross-correlation between v' and u'. Structure of $\overline{v'u'}$, normalized by their variances and averaged over intraseasonal periods shows that $\overline{v'u'} < 0$ (Fig. 5a), which implies a westward (eastward) eddy flux of southward (northward) momentum. And the correlation coefficient in frequency domain (Fig. 5b) indicates that the 20–40 day variability contributes substantially, particularly that in the lower pycnocline.

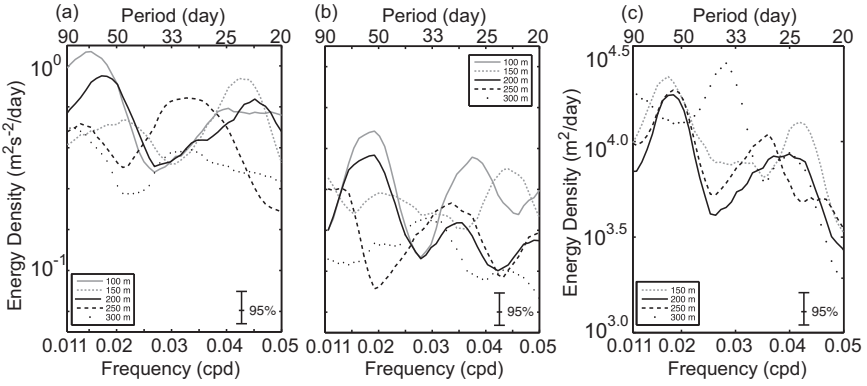

Fig. 4. Multitaper spectral estimate of u' and η' at several levels from Mak-West and Mak-East moorings within the lower thermocline of Makassar Strait during 2004–2006. (a) and (b) illustrate spectral estimate of u' for Mak-West and Mak-East respectively. (c) Displays η' spectral estimates of for Mak-West. Error bars on the spectral estimates mark the 95% confidence limits.

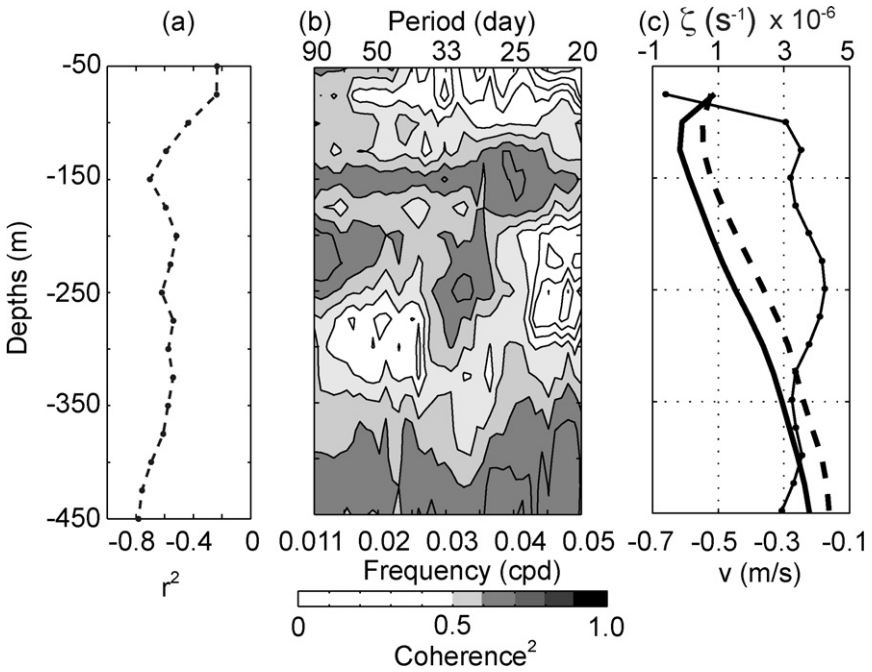

Fig. 5. (a) and (b) The degree of correlation between v' and u' at intraseasonal timescales over the Mak-West thermocline. (a) Zero-lag coefficients are obtained from time-lagged cross correlation analysis. (b) Amplitudes of coherence squared are shaded for values larger than 95% significance level. (c) Vertical structure of the background flow observed at Mak-West (solid line) and Mak-East (dashed line) and its corresponding relative vorticity (dotted line). The background flow at a certain depth is the time average of subinertial flow, which is obtained through applying a butterworth low-pass filter to the velocity field dataset with a cut-off period of 9.5-day (inertial period at the mooring site).

Another way to interpret $\overline{v'u'} < 0$ is in terms of the turbulence. The vertical structure of the mean flow (the time average of subinertial flow) observed at the Makassar Strait moorings indicates that the flow is directed southward and found with a maximum within the Mak-West pycnocline below 50 m (Fig. 5c). More energetic Mak-West flow yields positive mean zonal shear and relative vorticity ($\partial\overline{v}/\partial x > 0$). Assume that a particle at a point between Mak-West and Mak-East sites instantaneously moves eastward ($u' > 0$). The particle retains its original velocity during the migration, and when it arrives at Mak-East it finds itself in a region where a smaller velocity prevails. Thus the particle tends to speed up the neighboring fluid particles after it has reached the Mak-East site, and causes a more negative (southward) v'. Conversely, the particles that travel westward ($u' < 0$) tend to drag v' down. In this way turbulence tends to diffuse and attenuate the across gradient of the mean flow, $\partial\overline{v}/\partial x > 0$.

Another unique feature from u' varying at periods of 20–40 days, which is synonymously observed from both mooring, is a pattern of phase shift over depths: $u'(z+dz)$ tends to flow slower than $u'(z)$ with a constant lag. On a time and depth plot of u' at a 20–40 day period band (Fig. 6a), we draw lines, where each line connects the flow that has the same phase, i.e. phase lines. And those lines are uniformly tilted downward at an almost constant angle, indicative of a downward phase propagating feature. This downward phase shift found from u' differs from the phase shift of dominant variability in v'. Pujiana et al. (2009) suggested that the most dominant period band of v' observed in the Makassar Strait pycnocline exhibited upward phase propagation, which transferred energy downward to deeper depths at a speed of 25 m/day. A complex principal component (CPC) analysis of u' varying at timescales of 20–40 days indicates that up to 90% of variances can be explained by the first three eigenvectors, where the first mode describes 50% variance and the next two modes denote 25% and 15% variance respectively. From the eigenvector profile, we learn how the amplitudes of u' vary with depth. The first mode eigenvector reveals maxima at 175 m and at 250 m (Fig. 6b) where two distinct spectral peaks of

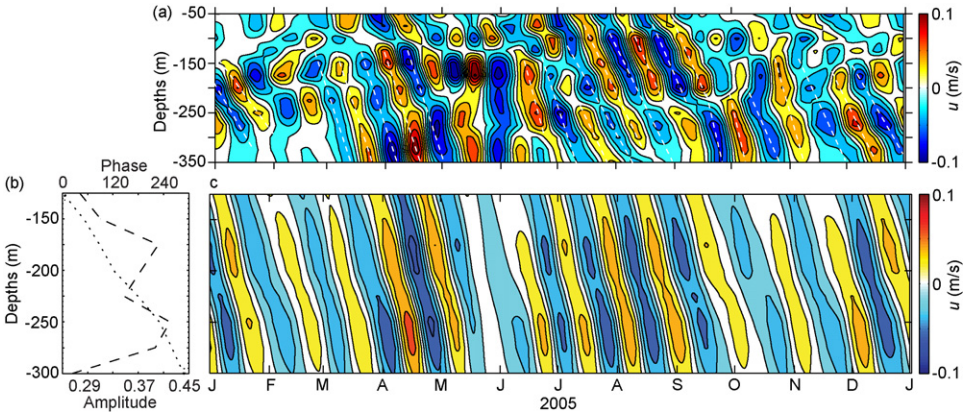

Fig. 6. Across-strait flow varying at periods of 20–40 days observed at Mak-West mooring in 2005 (a) and its orthogonal function approximation (b and c). Dashed lines in (a) show phase lines. Dashed and dotted lines in (b) show the 1st eigenvector and its relative phase that represents 50% variance of (a). (c) Reconstructed across-strait flow for the 1st mode.

25-day and 30-day are also observed: the energy associated with the spectral peak centered at 25-day is maximum at depth of 175 m, while the energy attributed to the 30-day variability is maximum at depth of 250 m. Therefore the vertical energy distribution for the 20–40 day across-channel flow is well resolved by the first eigenvector. Moreover, the relative phase inferred from the ratio between the imaginary and the real part of the first eigenvector signifies a phase increase with a rate of 1.7°/m towards greater depths (Fig. 6b). The rate of phase shift implies that it would take around 20 days for the 25-day oscillation to propagate from 125 m to 300 m of water column. This relative phase structure is better understood from reconstructed data obtained through a multiplication between eigenvectors and their corresponding principal components (time series). A plot of reconstructed u' based on eigenvector and principal component for the first mode captures the phase shift nature revealed by the eigenvector profile: periodic 20–40 day variability with phase lines titled downward at a uniform angle (Fig. 6c). Thus the unique downward phase propagation feature contained in the filtered 20–40 day u' data can be resolved and replicated by only the first mode.

3.1.2. Vertical displacement

The vertical displacement of the isotherms within Makassar Strait is rich in intraseasonal features (Fig. 4c). Fig. 4c demonstrates that significant variance associated with 25-day oscillation also characterizes temperature fluctuations at 150 m and greater depths. The vertical scale of the temperature variability within a period band of 20–40 days is likely larger than the lower pycnocline thickness, as the correlation between temperature variability at different depths shows that 70% temperature variance at 150 m is coherent with that at 300 m (not shown). Thermal field at intraseasonal timescales within Makassar Strait shares a similar power spectrum pattern with the across-strait flow data as the variability shows significant 20–40 day variation, and it is likely that the two parameters are physically linked.

3.1.3. Eddy-like features from observation

In previous sections we have discussed general characteristics of the 20–40 day variability in the Makassar Strait pycnocline extracted from datasets obtained at the Labani Channel of Makassar Strait. At least three interesting features attributed to the 20–40 day variability were obtained from the datasets.

1. The u' is more energetic than v' at depths extending from 100 m to 250 m. Although inferring the two-dimensional motion from two points is inherently tricky, we suspect that a dominant across-strait flow at the Labani Channel may relate to an eddy advected by the ITF. Assume an

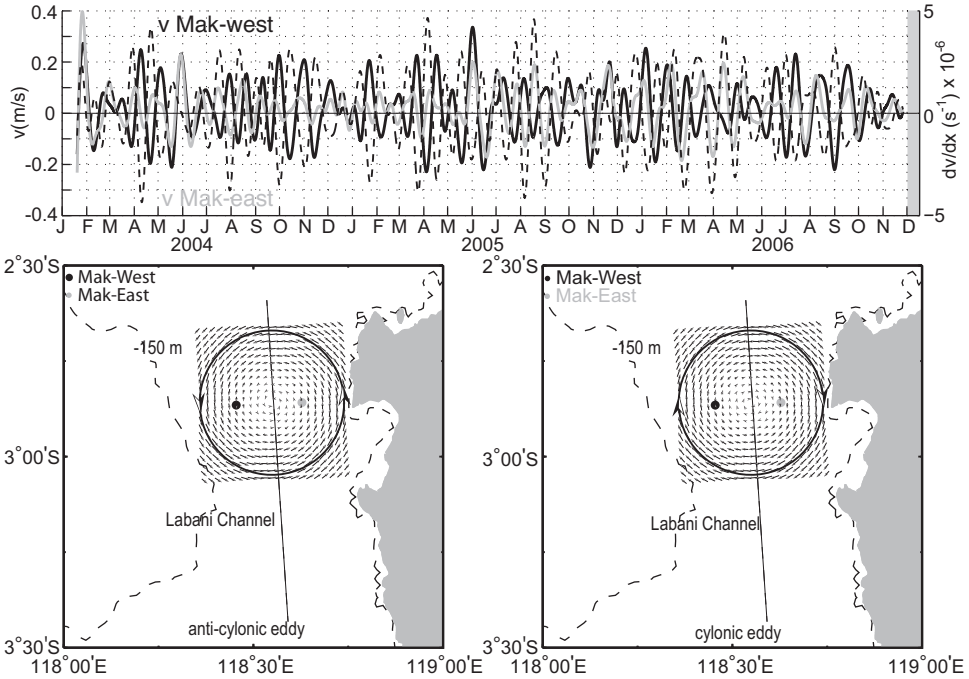

Fig. 7. (Upper panel): Along-strait flow varying at 20–40 days and observed at depth of 150 m of the Mak-west (black) and Mak-East (grey) thermocline and the corresponding dv/dx. (Lower panel): Illustration of ideal anticyclonic and cyclonic eddy currents in the Labani Channel. Dashed black line denotes the median line of the Labani Channel.

eddy propagates along a mean flow, $U(t)+iV(t)$, that is spatially uniform but varying with time, the eddy's path can be projected into a complex plane as $x'(t)+iy'(t)=r(t)e^{i\phi(t)}$. The currents observed by a mooring are then given as (Lilly and Rhines, 2002)

$$\xi(t) = V + iU - ie^{i\phi}\tilde{V}(r) \tag{1}$$

where is the radial velocity of the eddy and r is the distance from the mooring to the eddy center. If the eddy dynamics is simplified as a Rankine vortex, $\tilde{V}$ can be expressed in the following formula

$$\tilde{V}(r) = \begin{cases} VrR^{-1}, & r < R \\ Vr^{-1}R, & r > R \end{cases} \tag{2}$$

where V is the maximum azimuthal velocity, and R marks the eddy core radius that has uniform potential vorticity. Since the ITF flows in the y-direction at the Labani Channel, the observed eddy currents, by virtue of Eq. (1) and (2), then are always perpendicular to the along-strait axis or in the across-strait component. Therefore, the observed flow associated with the eddy would be more dominant in u' than in v'.

2. There are 17 $+\zeta'$ and 18 $-\zeta$' events over ~3 year observation at which the v' data in Mak-West and Mak-East moorings are in opposite directions: $+\zeta'$ occurs when $-v'$ at Mak-West and $+v'$ at Mak-East are observed, while $-\zeta'$ appears when $+v'$ at Mak-West and $-v'$ at Mak-East are observed (Fig. 7, upper panel). Given the Mak-West and Mak-East moorings are separated by a distance of ~19 km across a ~60 km width channel (Fig. 1b), the current vector in opposite senses that mark the positive and negative relative vorticity phases may imply that the moorings are located on different side of the passing eddies. To better visualize the relationship between the out of phase signature of v observed at the two moorings and an eddy, it is shown in Fig. 7 (lower panel) an ideal vortex, whose azimuthal velocity structure is given in Eq. (2), has a core with radius

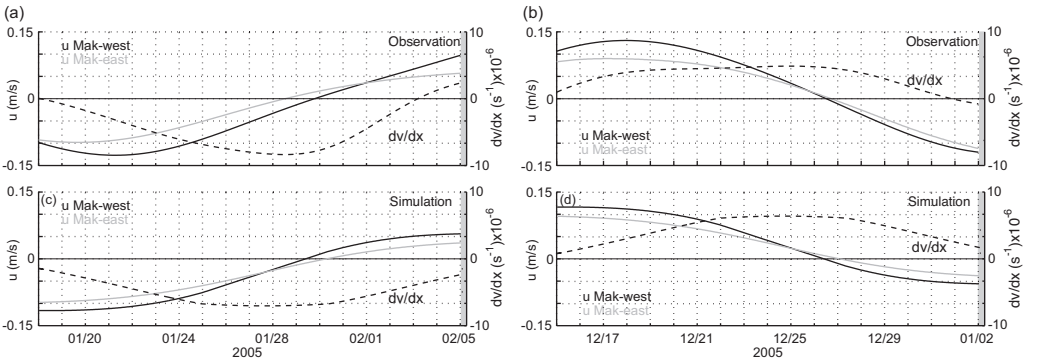

Fig. 8. Observation and simulation of across-strait flow (u) and relative vorticity (dv/dx) varying at 20–40 days at Mak-West and Mak-East mooring sites, which corresponds with anticyclonic and cyclonic eddy currents. (a and c) displays temporal variability of real and theoretical anticyclonic eddy respectively, while (b and d) demonstrates time series of observed and modeled cyclonic eddy respectively.

presumably of 20 km and its center assumed on the median line of the Labani Channel. It thus can be inferred from Fig. 7 (lower panel) that the out of phase nature shown by the v' timeseries at 20–40 days (Fig. 7, upper panel) may relate to eddies whose center likely occurs in between the two moorings.

3. The strongest $+\zeta$' episodes, at which $-v$' at both moorings is out of phase, are preceded with $+u$', while $-\zeta$' events coincide with initially observed $-u'$ (Fig. 8a and b). We argue that the relationship between u' and ζ' measured in the Labani Channel is consistent with what a mooring would observe from a passing eddy as suggested by Lilly and Rhines (2002): Normal component of eddy currents is initially positive (negative) for an anticlockwise (clockwise) eddy. To further examine whether the nature of u' is linked to eddy footprint at the moorings, we examine a Rankine vortex on Eulerian current records, which the associated currents can be written as

$$\xi(t) = \begin{cases} -iR^{-1}V\chi, & |\eta| < R \\ -i\chi^{*-1}VR, & |\eta| > R \end{cases} \tag{3}$$

where χ is the distance from the mooring location to the eddy center. We assume that V (the peak azimuthal speed at the eddy edge) is 15 cm/s, the southward advection speed of the vortex is 20 cm/s, the eddy core radius is 20 km, and the eddy center is set at about 31 km to the north of the measurement points for the initial condition. Also the isobaths are presumably perpendicular to the mooring transect, and the moorings are placed across a 50 km-wide channel in a way that replicates mooring arrangements in the Labani Channel. We run the eddy model with the same eddy parameters for both anticlockwise and clockwise eddies but change the sign of V from positive to negative for the clockwise eddy case. The simulated eddy currents, either for anticlockwise or clockwise eddy, yield a decent agreement with observations: the passing of a clockwise eddy ($-\zeta'$) is initially marked with westward currents ($-u'$) (Fig. 8c), while the occurrence of an anti-clockwise eddy ($+\zeta'$) is preceded by the onset of eastward currents ($+u'$) (Fig. 8d). A good accordance between real and theoretical events further indicates that the rotational events observed from moorings in the Labani Channel are likely related to eddy motions.

4. The thermal field and relative vorticity are linked at the Labani Channel. The isopycnals in the lower pycnocline layer dip down when the flow field exhibits negative relative vorticity (Fig. 9a). Meanwhile the isopycnals shoal as the relative vorticity observed in the Labani Channel lower pycnocline turns positive (Fig. 9b). We suspect that the vertical displacements of isopycnals varying at periods of 20–40 day in the lower pycnocline of the Labani Channel are direct responses to water column squeezing or stretching attributed to cyclonic or anti-cyclonic eddies, attributable to potential vorticity conservation. Potential vorticity conservation suggests that $(\zeta_{t0}+f)/h_{t0} = (\zeta_t+f)/h_t$, where

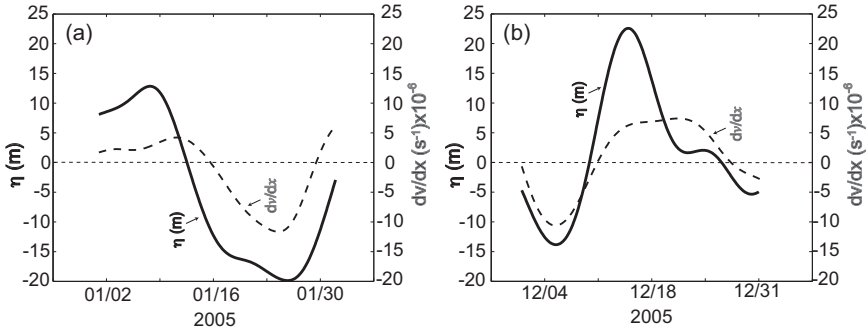

Fig. 9. Temporal variability of relative vorticity (dv/dx) and isotherm vertical displacement (η) at depth of 150 m observed from the moorings in the Labani Channel. (a) Demonstrates how a motion with $-dv/dx$ corresponds with a minimum η on 24 January 2005, while (b) illustrates the relationship between a $+dv/dx$ motion and a maximum η on 17 December 2005.

h is the isopycnal depth, and subscripts $t0$ and t denote initial condition (at rest) and time when an eddy passes the mooring sites. Assuming $\zeta_{t0} = 0$, h_t at the mooring sites located in the southern hemisphere can be written as $h_t = h_{t0}(1 - (\zeta_t/f))$, it can be inferred that the isopycnals are displaced upward (downward) when a motion with positive (negative) relative vorticity passes through the mooring sites or the pycnocline shoals (deepens) when an anticyclonic (cyclonic) eddy is advected through the observational sites.

After reviewing the observations discussed in previous sections, we hypothesize that the features attributed to the 20–40 day variability from the moorings at the Labani Channel are linked to eddy dynamics, and the next step is to describe where the eddies originate from. Several numerical experiments (Qiu et al., 1999; Masumoto et al., 2001) indicated that eddy activities at intraseasonal timescales are intense within the Sulawesi Sea, a basin located to the north of Makassar Strait (Fig. 1a). Masumoto et al. (2001) estimated that eddies with a period of 40-day were internally generated in Sulawesi Sea and affected the ITF transport in Makassar Strait. However the Sulawesi eddies that the study of Masumoto et al. (2001) numerically estimated were not only trapped in the lower pycnocline but rather occupied a thick water column extending from the surface to 1000 m isobath. To investigate the generating mechanism of eddies at the Labani Channel, we analyze the output of an eddy resolving numerical models in Makassar Strait, and the discussion is given in the following section.

4. The 20–40 day variability in an eddy-resolving model

As described earlier, flow and thermal field from two moorings at the Labani Channel of Makassar Strait reveal clear 20–40 day variability features, which we propose are related to cyclonic and anti-cyclonic eddies. To further examine the spatial variation and origin of the 20–40 day variability, we investigate the model output of a global HYCOM experiment (Metzger et al., 2010). We focus our analysis on the model flow at intraseasonal timescales in the Makassar Strait and Sulawesi Sea pycnocline. Comparison between the model output and observation at the Mak-West and Mak-East mooring sites indicates that the numerical experiment underestimates the Makassar Strait throughflow due to inaccurate model topography, where the Dewakang Sill (Fig. 1a), located near the southern end of the strait, was introduced 195 m too shallow in the model (Metzger et al., 2010). In addition to weaker simulated mean transport, the study of Metzger et al. (2010) also showed that shallower sill depth assigned in the model caused the maximum simulated southward flow in Makassar Strait to be ~50 m deeper than observed.

The model u' at intraseasonal timescales qualitatively agrees with observation at Mak-West and Mak-East moorings: the 20–40 day variability has clearly larger energy than other intraseasonal periods, and the variability at Mak-West is more energetic than that at Mak-East (Fig. 10a and b). It is also shown in Fig. 10a and b that the distinct monthly spectral peak is well simulated at depths greater

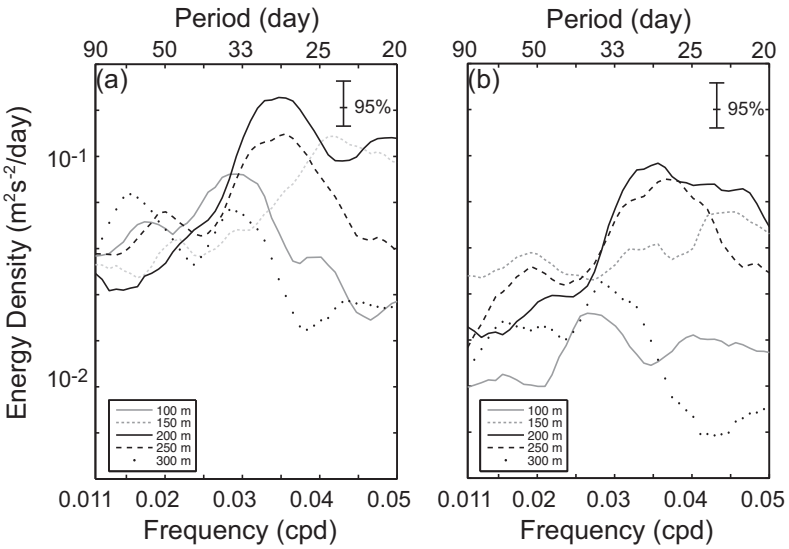

Fig. 10. Multitaper spectral estimates of simulated u' at intraseasonal timescales for several depths at the Mak-West (a) and Mak-East (b) locations in Makassar Strait. Error bars on the spectral estimates mark the 95% confidence level.

than 200 m, which is 50–75 m deeper than the depth where observation starts to record the monthly peak. The discrepancy is again due to inaccurate sill depth. Monthly variation also occurs in the model ζ' simulated at the mooring locations. Like the observation, the model ζ' and u' at depths beneath 200 m are linked: positive relative vorticity correlates with eastward flow, while negative vorticity corresponds with westward flow (not shown). A coherence analysis between the model ζ' and u' for several depths within the pycnocline layer of Mak-West site displays that both parameters varying at intraseasonal timescales are strongly coherent for a period band of 20–40 days, and the strongest correlation is found at depths greater than 200 m (not shown). Moreover the simulation not only qualitatively shows a good agreement with observation but also quantitatively explain significant variances of the recorded datasets. It is inferred from some cross-correlation analyses between the simulated and observed data at some select levels within the lower pycnocline depths that the model u' explains 64–72% variances of the observed u' varying at 20–40 days. Thus the numerical experiment is able to capture some general features of the 20–40 day variability, which are similarly revealed from observation at the mooring sites in the Labani Channel.

4.1. Eddy signature and its genesis in Makassar Strait

The next questions we explore within the model output are what causes the 20–40 day variability? Where does the forcing originate from? And why is the strong 20–40 day variability trapped within the lower pycnocline. To determine the ocean dynamics responsible for the pronounced 20–40 day fluctuations, the simulated flow field attributed to the period band of interest in the Makassar Strait is analyzed. We first want to gain insights on the space and time evolution of a motion that may drive the ζ' fluctuations in Makassar Strait. For example, an event of positive ζ' is inferred from two moorings at 250 m in the Labani Channel on 17 December 2005 (selected to be representative of positive ζ' events), and it is assumed that an anticlockwise eddy-like motion causes the ζ' field. The model agrees well with observation to simulate positive ζ' at 250 m of the Labani Channel pycnocline on 17 December 2005, and the model flow field shows that the positive ζ' value does correspond with a counter clockwise vortex motion with a diameter of ~40 km squeezed in the narrow Labani passage (Fig. 11). Assume quasi-geostrophic dynamics govern the vortex observed and simulated in the Labani Channel, the vortex diameter will be approximately as large as the local internal radius

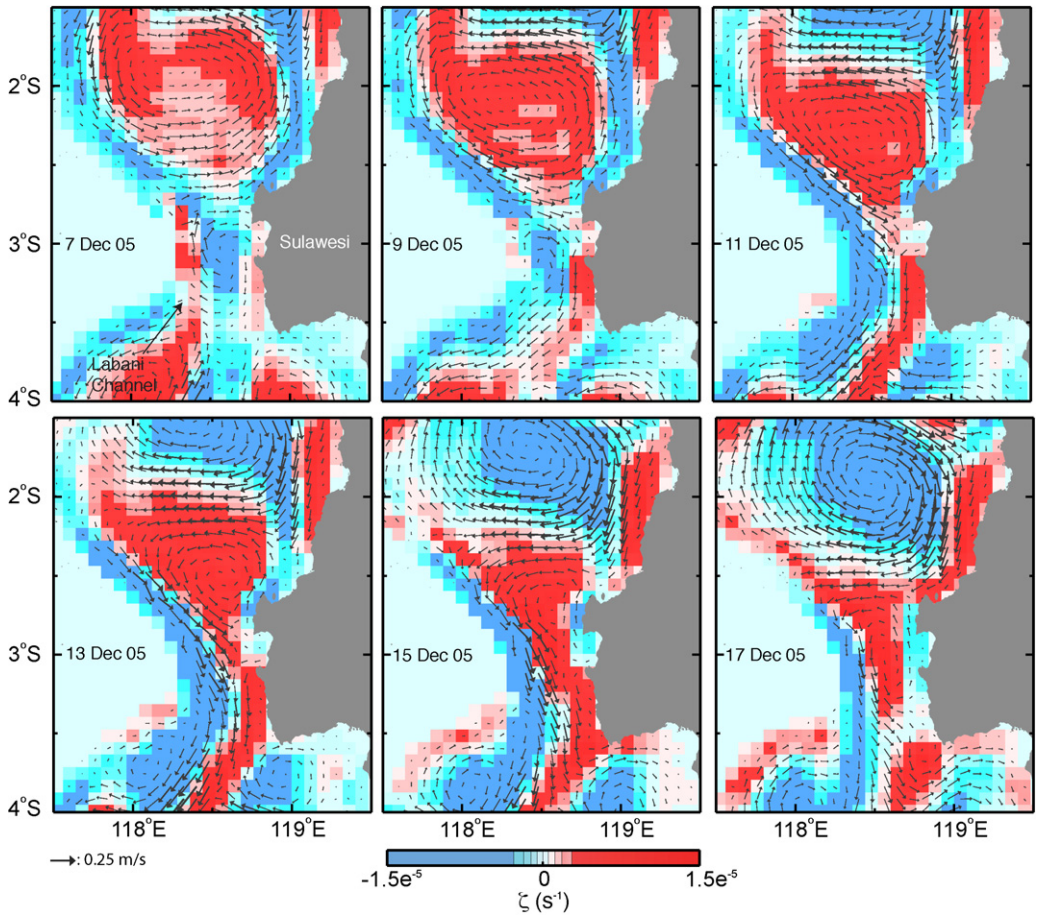

Fig. 11. Snapshots of the model horizontal flow field (arrow) and its corresponding vorticity field (in color) at 250 m in the vicinity of the Labani Channel for several days in December 2005. The current vectors are for periods of 20–40 days. The stars denote the mooring sites.

deformation, which is function of N, coriolis acceleration (f), and water depth (H). The deformation radius for the first oceanic mode in the Labani Channel falls within $O(\sim 275\,\text{km})$, substantially larger than the channel width itself. Therefore the eddy size in Makassar Strait is more likely topographically constrained. The model velocity and relative vorticity fields at the Labani Channel for over a period of

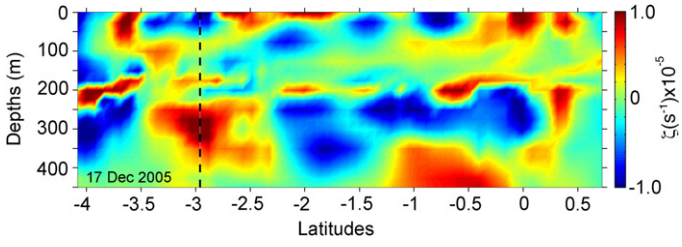

Fig. 12. The model ξ' plot for several depths along a transect in Makassar Strait shown in Fig. 1, simulated on 17 December 2005. The ζ' time series are computed using horizontal velocities for intraseasonal timescales. The dashed line indicates the latitude of the mooring location in the Labani Channel.

~3 years (2004–2006) display 23 events of anti-cyclonic vortex motion and 17 episodes of cyclonic eddy-like features.

Furthermore, following the spatial and temporal eddy core variability, it can be inferred that the eddy-like motion is not locally generated at the Labani Channel but seems rather to propagate from the northern Makassar Strait into the Labani Channel. It is shown in Fig. 11 that an anti-cyclonic eddy with a diameter of ~100 km has its core located at latitude of 2°S and is simulated on 7 December 2005, and the eddy diameter is reduced as it propagates southward with a phase speed of 0.25 m/s before occupying the Labani Channel on 17 December 2005. After reaching the Labani Channel, the eddy dissipates and its signature is not simulated further south (not shown).

The model eddy occurs only within the lower pycnocline and is identifiable as a feature that has homogeneous ζ' over depths. A depth versus distance plot of ζ' along a transect given in Fig. 1 shows that a homogeneous positive ζ' over depths extending from 200 to 350 m marks the event of an anti-cyclonic eddy on 17 December 2005 in the Labani Channel (Fig. 12). Thus the eddy varying at periods of 20–40 days in Makassar Strait is trapped within the lower pycnocline. Several snapshots of simulated horizontal flow fields and structure of ζ' in Makassar Strait (Figs. 11 and 12) provide

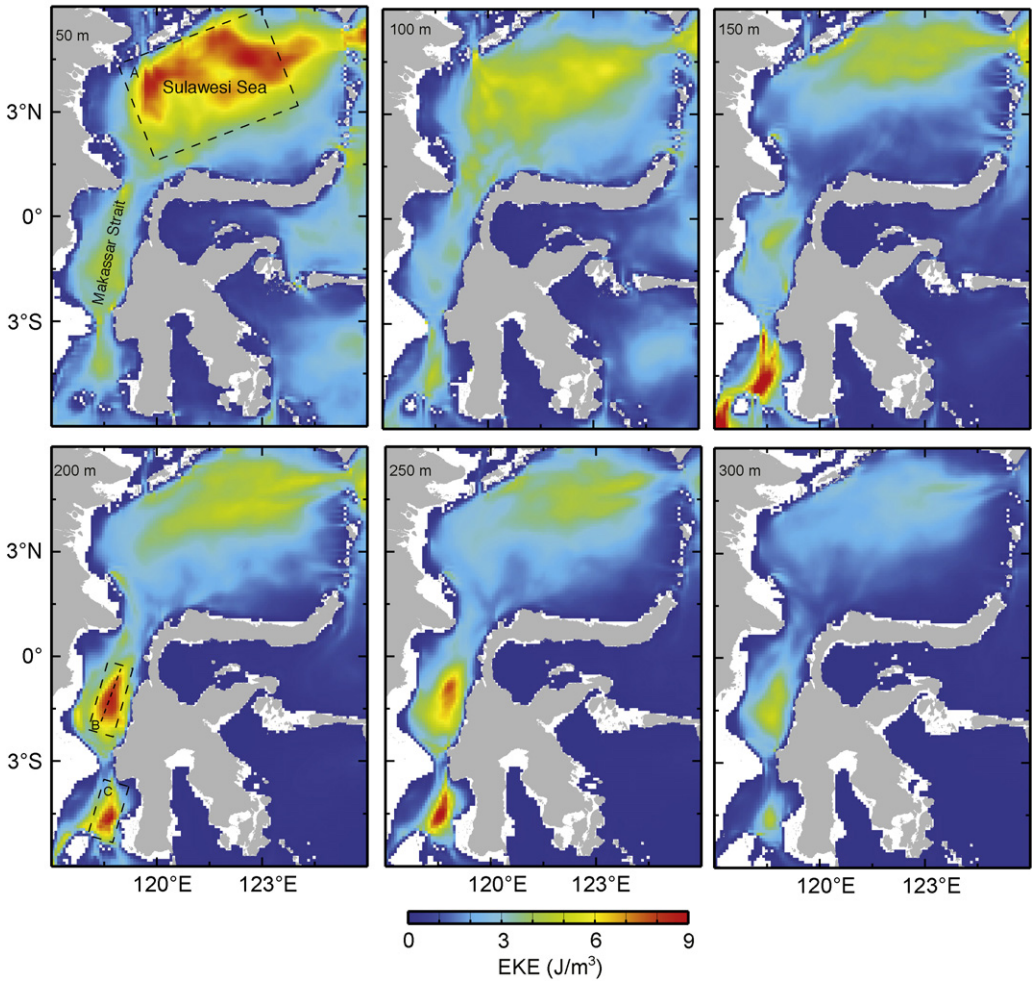

Fig. 13. Plots of the averaged EKE simulated at several depths within the Makassar Strait and Sulawesi Sea thermocline. The mean EKE is computed for a 3-year period from 2004 to 2006. Dashed box represents a region with the most energetic EKE.

spatial and temporal dimension of the motions that likely force the 20–40 day variability observed at the Labani Channel. It is shown that circular motions develop at 2°S or farther north and propagate southward in Makassar Strait. To better map out the source region of the vortices, we analyze simulated eddy kinetic energy (EKE) budget over an expanded region including the Sulawesi Sea (Fig. 1), a basin with robust intraseasonal activities (Qiu et al., 1999; Masumoto et al., 2001, Pujiana et al., 2009). Although detecting energy radiation through EKE can be ambiguous, the intraseasonal variability can be characterized by a suitably specified EKE.

The EKE budget is deduced from the rapidly-varying segment of u and v, with an assumption that each variable has a slowly-varying part and a rapidly-varying part, labeled as (u, v) and (u', v') respectively. The rapidly-varying part oscillates at periods of 20–40 days, and the EKE density is therefore defined as $0.5\rho_o(u'^2 + v'^2)$, where ρ_o is the background density, vertically averaged over depths from the potential density structure given in Fig. 2. Comparison of the averaged EKE (Fig. 13) at several depths clearly exemplifies the basins with the most pronounced EKE in the region: Sulawesi Sea (A), northern Makassar Strait (B), and Southern Makassar Strait (C), where the Labani Channel demarcates the separation between the northern and southern of Makassar Strait. Nevertheless we consider basins A and B as the only viable energy source areas for eddy activities at the Labani Channel as we expect the eddy to be advected, along with the ITF, southward into the channel. In area A, the eddy activity is significant close to the surface and decays away from it, and the eddy likely does not extract its energy from the wind because the atmospheric perturbations over the area lacks a 20–40 days variability (not shown). The eddy might instead relate to instabilities of the Mindanao currents occurring on the eastern Mindanao coasts or be a Sulawesi basin scale response to the periodic Mindanao currents (Qiu et al., 1999; Masumoto et al., 2001). In contrast, the EKE vertical distribution in B shows a structure that is quite typical of the mean flow profile in the Labani Channel (Fig. 5c), in which the maximum value is attained at the mid pycnocline depth, where the vertical shear of the mean flow is strongest. The EKE in B is strongest at 200 m and fades away with distance from that depth (Fig. 14a).

Considering how the EKE is distributed in Makassar Strait and Sulawesi Sea, we propose that zone B, rather than area A in Sulawesi Sea, is the EKE source for generating eddies that are trapped in the lower pycnocline and propagate into the Labani Channel. If area B were the eddies source, southward dispersion of EKE should be well simulated by the model. To detect if there is southward energy transfer from zone B, we evaluate the time evolution of EKE at a depth of 225 m, a depth that has the largest averaged EKE value (Fig. 14a). The EKE temporal variability along a band of latitudes within zone B demonstrates a southward propagating with a phase speed of 0.2 m/s which closely matches the propagation speed of an eddy (Fig. 14b). To a first approximation, it therefore can be proposed that the eddy observed in the Labani Channel is not generated in the Sulawesi Sea, but rather originating from just to the north of the channel in the Makassar Strait at latitudes varying from 0.5°S to 2°S.

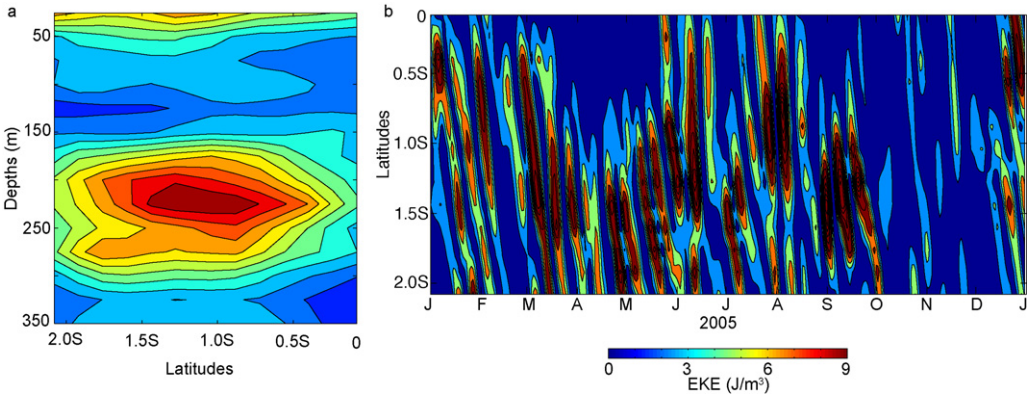

Fig. 14. (a) A vertical distribution plot of the mean EKE simulated at several latitudes within zone B given in Fig. 13. (b) The temporal variability of the model EKE at depth of 250 m for several latitudes along a transect within zone B shown in Fig. 13.

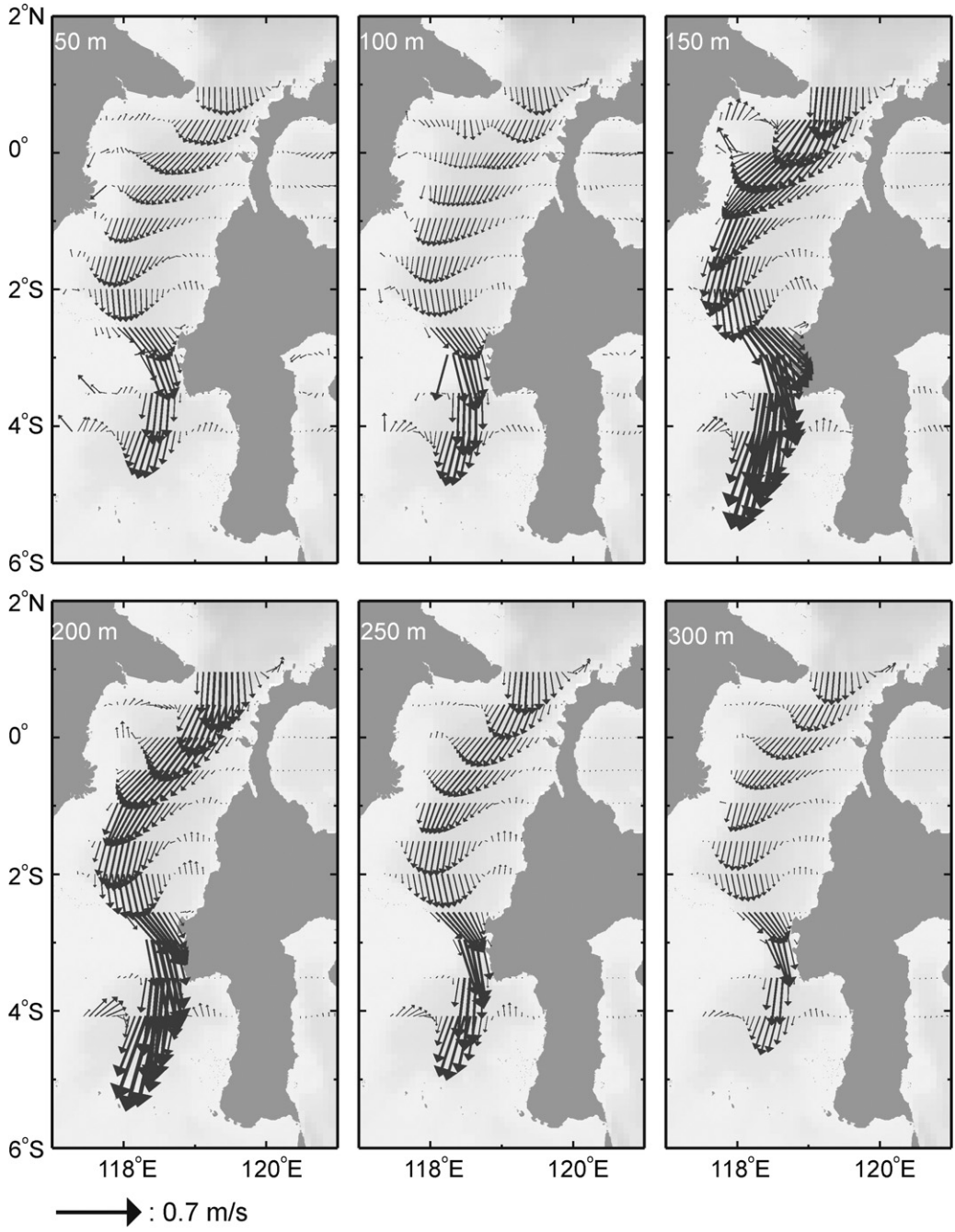

Fig. 15. The model background flow at several depths simulated in the Makassar Strait thermocline. The mean flow is obtained through applying a butterworth low-pass filter to the model raw data with a cutoff period of 90-day.

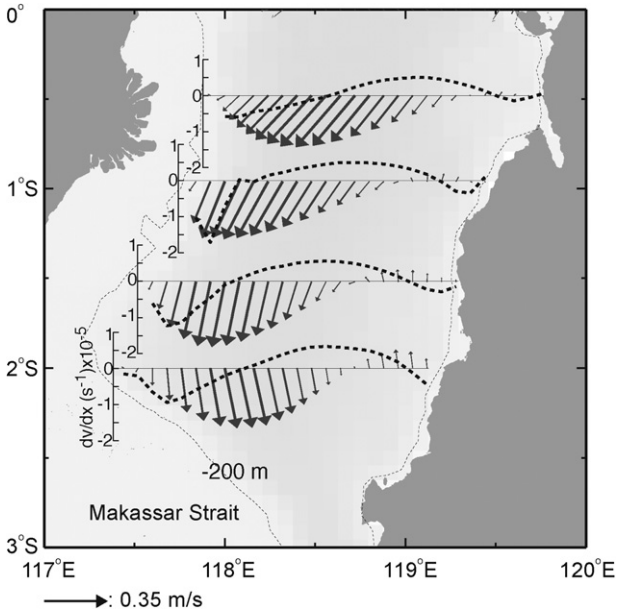

Fig. 16. The model background flow and relative vorticity at depth of 200 m simulated within latitudes of 0.5°–2°S. The mean flow is obtained through applying a butterworth low-pass filter to the model raw data with a cutoff period of 90-day.

The next questions are why the eddy-like motions are formed at latitudes which fall within range of 0.5°–2°S in the Makassar Strait lower pycnocline, and how are they initiated? As mentioned in the earlier discussion on eddies characteristics from observation, we argue that the eddy occurring at depths beneath the mid pycnocline layer of Makassar Strait extracts its energy from the sheared mean flow. To support the argument that the eddy generation may relate to the background flow, spatial variation of the time averaged speeds in Makassar Strait at several depths within the pycnocline, is studied. The background flow magnitudes at several different depths (Fig. 15) synonymously display significant variations across Makassar Strait: the southward mean flow is simulated speediest at and south of the Labani Channel and at depths of 150–200 m. Fig. 15 also demonstrates a clear across-strait gradient of the mean flow particularly at latitudes of 0.5°–2°S as weaker northward mean flow on the eastern end of the Makassar Strait features against the energetic western-intensified southward mean flow. And the across-strait gradient of the mean flow within that particular latitude band reveals its maximum at 200 m, a depth where the EKE is noticeably largest as shown in Fig. 13. Given the sheared mean flow and the EKE equally exhibit strongest signature at depth of 200 m, we propose that the background flow supplies the eddy energy through a flow instability mechanism. Assuming the mean flow structure across the strait can be described as an inviscid parallel flow, the two necessary criteria for instability of the flow are: the basic background flow profile has at least a point of inflection (Rayleigh's inflection point criterion), and the magnitude of vorticity of the background flow must have a maximum within the region of flow, not at the boundary (Fjortoft's theorm). The imaginary part of the Rayleigh's equation (Kundu and Cohen, 2004), $c_i \int(\partial^2 V/\partial x^2|\phi|^2/|V-c|^2)dx = 0$, suggests that for the unstable case to hold ($c_i \neq 0$), $\partial^2 V/\partial x^2$ (the mean flow curvature) needs to change sign across the strait (x-direction). Focusing on the across-strait profile of the mean flow at 200 m within latitudes of 0.5°–2°S in Makassar Strait (Fig. 16), the profile shows one inflection point at each latitude that marks the mean flow structure across the strait, which complies with the necessary criterion for instability required by the Rayleigh's equation. Another criterion for instability derived from Fjortoft's theorem (Kundu and Cohen, 2004), $\int(\partial^2 V/\partial x^2(V-V_I)|\phi|^2/|V-c^2|)dx < 0$, indicates that the mean flow must not only have at least one inflection point across the strait but also have maximum vorticity away from the boundary. And Fig. 16 also demonstrates that the positive relative vorticity magnitude

of the mean flow has a maximum within the region of flow, which provides another indication that the background flow instability simulated within latitudes of 0.5°–2°S in Makassar Strait potentially generate the eddies.

5. Discussion and summary

We have described the characteristics of the 20–40 day variability observed at the two INSTANT moorings deployed in the Labani Channel of Makassar Strait 2004–2006. The variability is well identified from the u' datasets recorded below the central pycnocline depth of 125 m, as a distinct spectral peak, which resembles a blue spectrum shape over the intraseasonal timescales. Comparison between u' and v' demonstrates that the across-strait component of the 20–40 day variability intraseasonal feature is more energetic within the pycnocline. Additionally, the 20–40 day fluctuations of u' reveal downward phase propagation with a speed of 25 m/day and vertical distribution of energy, in which the flow at the mid pycnocline depth oscillates at shorter period than it does at greater depths.

Apart from u', the 20–40 day variability is also evident from the temperature datasets as η' continuously show monthly periodicity. The magnitude of η' is larger than the lower pycnocline thickness, and η' move up and down in concert although a small phase difference is observed over the lower pycnocline layer. Although the 20–40 day variability is not prominent in v', it does typify the $\partial v'/\partial x$ variation over the lower pycnocline depths. The $\partial v'/\partial x$ time series exhibit strong correlations with u' which leads us to propose that the 20–40 day variability is linked to eddy-like features. As discussed previously, the velocity structure of a theoretical vortex approximates well the observations and the relationship between the measured parameters. Moreover the link between ζ' and η', the isopycnals dip down (elevated) as the relative vorticity magnitudes turn negative (positive) may also signify the presence and role of an eddy to conserve the potential vorticity within the water column in the Labani Channel.

If an eddy forces the 20–40 day variability within the lower pycnocline layer, why does the variability at the top of the lower pycnocline has strongest energy at a period of 25-day while the variability at the base of the lower pycnocline attains maximum energy at a period of 30-day? In other word, the spectral peak attributed to the 20–40 day variability is centered at periods varying from 25-day at the mid pycnocline depth to 30-day at the base of the lower pycnocline depth. Here, we suggest a Doppler effect may better explain the pattern in question than the motion's natural frequencies. Referring to the general dispersion relation for gravity waves, natural frequencies of motions that a strait inherently can sustain is inversely proportional to the strait's width, $\omega = ((\pi g(n+1)L^{-1})\tanh((n+1)\pi HL^{-1}))^{1/2}$ where H, L, g, and n denote water depth, strait's width, gravity and mode number, respectively. The relationship between the natural frequency and the strait's width thereby indicate that as strait's width decreases with depth, natural frequencies (periods) would get larger (smaller) with depth as natural frequency is inversely proportional to strait's width. However, this increasing natural frequency with narrower width relationship does not fit well in the Labani Channel because the dominating frequency gets smaller as the channel's width decreases with depth. Another physical process that may explain increasing periods of fluctuations with depth is Doppler phase shift. If the 20–40 day event is advected southward with the background flow, the feature is advected into the mooring sites with varying speeds over depths, following the vertical structure of the mean flow (Fig. 5c), which is maximum at the mid pycnocline depth and decays with distance from this depth. As consequence, the observed dominant period of oscillation at the mid pycnocline depth is shorter than that at deeper levels in which the 20–40 day variability propagates at a slower pace.

An eddy-resolving model further supports that the 20–40 day variability observed in the Labani Channel of Makassar Strait is driven by eddies. The model horizontal flow and ζ' fields show that a positive (negative) ζ' event observed in the channel does correspond with an anti-cyclonic (cyclonic) eddy that originates in Makassar Strait at latitudes between 0.5° and 2°S, just to the north of the mooring site, a region with the largest EKE. The EKE vertical distribution within this band of latitudes demonstrates strongest EKE magnitude at depths greater than 200 m. The area and depths with the largest EKE also coincides with the latitudes and levels at which the across-strait gradient of the model background flow may provide the necessary energy for the eddy formation in Makassar Strait.

To summarize, we suggest that a cyclonic or an anti-cyclonic eddy generated at latitudes between 0.5° and 2°S in Makassar Strait explains strong signatures of the 20–40 day variability in the across-strait flow and the temperature fluctuations observed within the lower pycnocline of the Labani Channel. The generation mechanism of the eddy is likely through instability in which the required energy is supplied by the across-strait shear of along-strait flow, marking the ITF. The eddy is trapped in the lower pycnocline because those are depths the EKE and the sheared background flow is found most energetic. The eddy propagates southward along with the ITF and dissipates its energy in the Labani Channel.

Acknowledgements

This work is supported by the National Science Foundation grant OCE-0219782, OCE-0725935, and OCE-0725561. Bruce Huber is acknowledged for helping the preparation of gridded current datasets. The HYCOM component of this article is a contribution from the "6.1 Dynamics of the Indonesian Throughflow (ITF) and Its Remote Impact" project sponsored by the Office of Naval Research under program element number 61153 N. Grants of computer time were provided by the Department of Defense (DoD) High Performance Computing Modernization Program and the simulations were performed on the IBM Power 4+ (Kraken), the IBM Power 6 (daVinci) and the Cray XT5 (Einstein) at the Navy DoD Supercomputing Resources Center, Stennis Space Center, MS. This is Lamont-Doherty contribution number 7517 and NRL contribution NRL/JA/7320–11-7364. This publication has been approved for public release and distribution is unlimited.

References

Gordon, A.L., Kamenkovich, V.M., 2010. Modelling and observing the Indonesian throughflow. A special issue of dynamics of atmosphere and ocean. Dyn. Atmos. Oceans, doi:10.1016/j.dynatmoce.2010.04.003.

Gordon, A.L., Sprintall, J., Van Aken, H.M., Susanto, D., Wijffels, S., Molcard, R., Ffield, A., Pranowo, W., Wirasantosa, S., 2010. The Indonesian throughflow during 2004–2006 as observed by the INSTANT program. Dyn. Atmos. Oceans, doi:10.1016/j.dynatmoce.2009.12.002.

Gordon, A.L., Susanto, R.D., 1999. Makassar Strait transport: initial estimate based on Arlindo results. Mar. Tech. Society 32, 34–45.

Gordon, A.L., Fine, R.A., 1996. Pathways of water between the Pacific and Indian Oceans in the Indonesian seas. Nature 379, 146–149, doi:10.1038/379146a0.

Gordon, A.L., Susanto, R.D., Ffield, A., Huber, B.A., Pranowo, W., Wirasantosa, S., 2008. Makassar Strait throughflow, 2004 to 2006. Geophys. Res. Lett. 35, L24605, doi:10.1029/2008GL036372.

Kundu, P.K., Cohen, I.M., 2004. Fluid Mechaniscs. Elsevier, New York.

Lilly, J.M., Rhines, P.B., 2002. Coherent Eddies in the Labrador Sea Observed from a Mooring. J. Phys. Oceanogr. 32, 585–598, doi:10.1175/1520 0485(2002)032<0585:CEITLS>2.0.CO;2.

Masumoto, Y., Kagimoto, T., Yoshida, M., Fukuda, M., Hirose, N., Yamagata, T., 2001. Intraseasonal eddies in the Sulawesi Sea simulated in an ocean general circulation model. Geophys. Res. Lett. 28 (8), 1631–1634.

Metzger, E.J., Hurlburt, H.E., Xu, X., Shriver, J.F., Gordon, A.L., Sprintall, J., Susanto, R.D., Van Aken, H.M., 2010. Simulated and observed circulation in the Indonesian seas: 1/12(Global HYCOM and the INSTANT observations. Dyn. Atmos. Oceans 57, 275–300, doi:10.1016/j.dynatmoce.2010.04.002.

Pujiana, K., Gordon, A.L., Sprintall, J., Susanto, R.D., 2009. Intraseasonal variability in the Makassar Strait thermocline. J. Mar. Res. 67, 757–777.

Qiu, B., Mao, M., Kashino, Y., 1999. Intraseasonal variability in the Indo-Pacific throughflow and the regions surrounding the Indonesian seas. J. Phys. Oceanogr. 29, 1599–1618, doi:10.1175/1520-0485(1999)029<1599:IVITIP>2.0.CO;2.

Susanto, R.D., Gordon, A.L., Sprintall, J., Herunadi, B., 2000. Intraseasonal variability and tides in Makassar Strait. Geophys. Res. Lett. 27 (10), 1499–1502, doi:10.1029/2000GL011414.

Sprintall, J., Wijffels, S., Gordon, A.L., Ffield, A., Molcard, R., Susanto, R.D., Soesilo, I., Sopaheluwakan, J., Surachman, Y., Van Aken, H., 2004. INSTANT: a new international array to measure the Indonesian throughflow. Eos Trans. AGU 85 (39), doi:10.1029/2004EO390002.